



HAL
open science

Micromechanical modelling of intracellular pressure-induced deformation of foams; application to expanded polystyrene

Teddy Fen-Chong, Eveline Hervé-Luanco, André Zaoui

► **To cite this version:**

Teddy Fen-Chong, Eveline Hervé-Luanco, André Zaoui. Micromechanical modelling of intracellular pressure-induced deformation of foams; application to expanded polystyrene. *European Journal of Mechanics - A/Solids*, 1999, 18 (2), pp.201-218. 10.1016/S0997-7538(99)80012-6 . hal-00111617

HAL Id: hal-00111617

<https://hal.science/hal-00111617v1>

Submitted on 9 Nov 2022

HAL is a multi-disciplinary open access archive for the deposit and dissemination of scientific research documents, whether they are published or not. The documents may come from teaching and research institutions in France or abroad, or from public or private research centers.

L'archive ouverte pluridisciplinaire **HAL**, est destinée au dépôt et à la diffusion de documents scientifiques de niveau recherche, publiés ou non, émanant des établissements d'enseignement et de recherche français ou étrangers, des laboratoires publics ou privés.



Distributed under a Creative Commons Attribution - NonCommercial 4.0 International License

Micromechanical modelling of intracellular pressure-induced viscoelastic shrinkage of foams: application to expanded polystyrene

Teddy Fen-Chong, Eveline Hervé, André Zaoui*

Laboratoire de Mécanique des Solides – CNRS, École Polytechnique, 91128 Palaiseau, France

Expanded polystyrene (EPS) beads have a cellular microstructure with closed cell membranes made of polystyrene. After demoulding, the intracellular temperature and pressure decrease down to room temperature and to atmospheric pressure. It is here shown that after processing, EPS shrinkage and after-shrinkage can be partly correlated to the intracellular pressure decrease, assuming that polystyrene is viscoelastic. To do so, use is made of micromechanical techniques in non-isothermal, linear, non-ageing viscoelasticity.

micromechanics / viscoelasticity / foams / expanded polystyrene / shrinkage

1. Introduction

Expanded polystyrene (EPS) slabs show time-dependent deformation after manufacturing. This deformation can last from days to months. Until 6 weeks after manufacturing its amount can be high enough to prevent EPS panels from being used as a core material in composite elements for building applications. Consequently, such an industrial application demands foamed polystyrene to be kept in stock for stabilization, which could be avoided through a better understanding of the shrinkage mechanisms.

Järvelä et al. (1986) made a phenomenological analysis of this question. They studied the influence of some manufacturing parameters on the dimensional variations as observed on moulded EPS in order to reduce their amount and to quicken their rate (i.e., to shorten their duration). However, this phenomenological approach is not appropriate to separate the influence of the physical processes which act at the scale of the EPS cellular microstructure after manufacturing. From this processing step it can be useful to first understand what happens inside an isolated bead and to model its mechanical behaviour in view of performing a structural analysis of an EPS slab, which will next combine the material properties and the moulding heterogeneities. The former stage is typically the concern of micromechanics, and the latter is out of the scope of this paper.

The considered EPS is made from beads of polystyrene containing dispersed particle-like blowing agents such as pentane. After the temperature has been raised above the boiling point of pentane and in the range of polystyrene glass transition, each bead expands and acquires a cellular microstructure as shown in *figure 1*. Following this pre-expansion, EPS slabs are produced by further expansion of a great number of pre-expanded beads in a mould. After demoulding, the temperature inside the slab is spatial- and time-dependent until it reaches room temperature. There exists an overpressure (relative to the atmospheric one) inside each cell, which is likely to be one of the important physical parameters influencing the dimensional variations of EPS beads and thus of EPS slabs.

* Correspondence and reprints

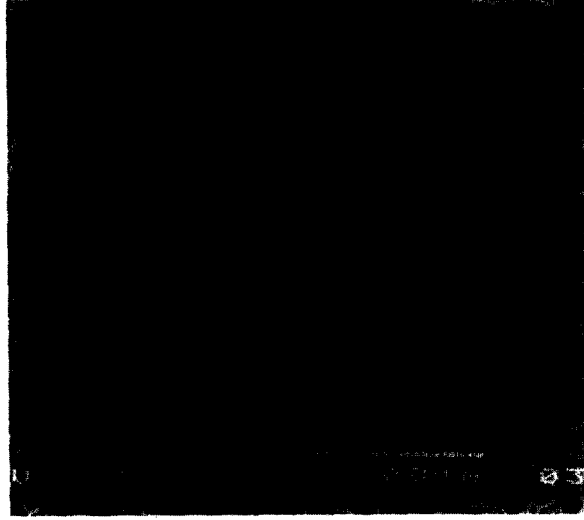


Figure 1. Cellular microstructure of an isolated EPS bead (scanning electron micrograph): the cell membranes of polystyrene appear in white and the porous cells in grey.

Each EPS bead, considered as the foamed polystyrene representative volume element, exhibits closed cells (i.e., each cell is sealed off from its neighbours by membranes), the thermo-mechanical behaviour of which depends on that of the cell membranes made of polystyrene, on the porosity and on the intracellular pressure. As the temperature varies from 373 K to room temperature, one has to deal with non-isothermal conditions.

Before predicting this anisothermal and time-dependent overall behaviour of an EPS bead after demoulding, we first address the problem of deriving the intracellular pressure-induced strain tensor of any foam with closed cells. This is done in small strains from Section 2 to Subsection 4.2.

To do so, use is made of classical homogenization techniques for linear elasticity in Section 2: the micromechanical treatment uses a local pre-stress field representing the intracellular pressure in a heterogeneous material, and the latter is not actually coupled with cell deformation. It is then possible to determine the overall strain of a volume element of foam with closed cells, the dependence of which on the intracellular pressure, the cellular microstructure and the cell membranes elastic moduli follows from the use of the ‘porous’ isotropic three-phase model (Hervé and Zaoui, 1993; Hervé and Pellegrini, 1995). In Section 3, the micromechanical treatment is extended to linear and non-ageing isothermal viscoelasticity by use of the correspondence principle (Mandel, 1955) whereas in Section 4, this situation is generalized to non-isothermal conditions (Morland and Lee, 1960; Muki and Sternberg, 1961; Christensen, 1971). From Subsection 4.2, some hypotheses are introduced in order to determine the EPS bead time-dependent deformation. When the temperature has reached room temperature, the EPS after-shrinkage is evaluated (Section 5).

2. Micromechanical modelling in linear elasticity

2.1. Overall strain of a heterogeneous body with a pre-stress field

The considered problem, (P) in *figure 2*, is that of deriving the overall strain $\underline{\underline{E}}$ of a heterogeneous elastic body occupying a domain Ω , subjected to a non-equilibrated pre-stress field $\underline{\underline{\sigma}}^p(\underline{x})$ and to a prescribed homogeneous stress $\underline{\underline{\Sigma}}$ at its boundary $\delta\Omega$. The elastic moduli $\underline{\underline{C}}(\underline{x})$ and compliances $\underline{\underline{S}}(\underline{x})$ vary with position, \underline{x} .

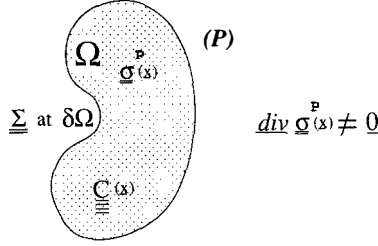


Figure 2. Heterogeneous body with a non-equilibrated pre-stress field $\underline{\underline{\sigma}}^p(x)$. The uniform stress $\underline{\underline{\Sigma}}$ is prescribed at its boundary.

Let $\underline{\underline{\sigma}}(x)$ be the resulting stress field. Its spatial average over Ω equals the prescribed stress $\underline{\underline{\Sigma}}$ at the boundary

$$\underline{\underline{\Sigma}} = \langle \underline{\underline{\sigma}}(x) \rangle_{\Omega} \quad (1)$$

and the same relation holds for the strain

$$\underline{\underline{E}} := \langle \underline{\underline{\varepsilon}}(x) \rangle_{\Omega} \quad (2)$$

We can analyse this problem (P) as the superposition of two elementary problems (P') and (P'') (figure 3). Problem (P') is a classical heterogeneous elastic problem of a body in a natural state and subjected to the same uniform stress $\underline{\underline{\Sigma}}$ as in problem (P) at its boundary. This body has identical moduli and compliances to those in problem (P). In problem (P''), the body is the same as in problem (P), but has been unloaded at its boundary. We have, with obvious notations

$$\underline{\underline{\varepsilon}}(x) = \underline{\underline{\varepsilon}}'(x) + \underline{\underline{\varepsilon}}''(x) \quad (3)$$

$$\underline{\underline{E}} = \langle \underline{\underline{\varepsilon}}'(x) \rangle_{\Omega} + \langle \underline{\underline{\varepsilon}}''(x) \rangle_{\Omega} \quad (4)$$

The second part of the right-hand member of (4) is the overall strain $\underline{\underline{E}}''$ of the pre-stressed body after unloading ($\underline{\underline{\Sigma}} = \underline{\underline{0}}$) or the overall residual strain in (P) as well, while the first part of the right-hand member of (4) is the overall elastic strain $\underline{\underline{E}}^{el}$ of the body in problem (P') [or (P)] and is given by

$$\underline{\underline{E}}^{el} := \langle \underline{\underline{\varepsilon}}'(x) \rangle_{\Omega} = \underline{\underline{S}}^{hom} : \underline{\underline{\Sigma}} \quad (5)$$

where $\underline{\underline{S}}^{hom}$ is the overall elastic compliance.

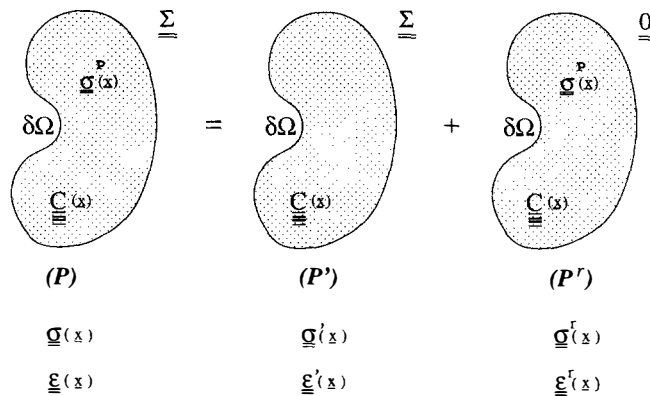


Figure 3. Decomposition of the problem (P) into two elementary problems (P') and (P'').

Due to linearity, the stress field $\underline{\underline{\sigma}}'(\underline{x})$ is linearly related to the prescribed stress $\underline{\underline{\Sigma}}$ by a stress-concentration tensor $\underline{\underline{B}}(\underline{x})$

$$\underline{\underline{\sigma}}'(\underline{x}) = \underline{\underline{B}}(\underline{x}) : \underline{\underline{\Sigma}} \quad (6)$$

The overall elastic compliance $\underline{\underline{S}}^{hom}$ is, as usual, given by

$$\underline{\underline{S}}^{hom} = \langle \underline{\underline{S}}(\underline{x}) : \underline{\underline{B}}(\underline{x}) \rangle_{\Omega} \quad (7)$$

with

$$\langle \underline{\underline{B}}(\underline{x}) \rangle_{\Omega} = \langle {}^t \underline{\underline{B}}(\underline{x}) \rangle_{\Omega} = \underline{\underline{I}} \quad (8)$$

where ${}^t \underline{\underline{B}}(\underline{x})$ is the transposed of $\underline{\underline{B}}(\underline{x})$ and $\underline{\underline{I}}$ is the fourth-rank identity tensor; $I_{ijkl} := \frac{1}{2}(\delta_{ik}\delta_{jl} + \delta_{il}\delta_{jk})$. Since $\underline{\underline{\sigma}}'(\underline{x})$ is statically admissible with $\underline{\underline{\Sigma}}$, we have

$$\underline{\underline{\Sigma}} = \langle \underline{\underline{\sigma}}'(\underline{x}) \rangle_{\Omega} \quad (9)$$

In problem (P^r) the stress $\underline{\underline{\sigma}}^r(\underline{x})$ and strain $\underline{\underline{\epsilon}}^r(\underline{x})$ are related to each other by

$$\underline{\underline{\epsilon}}^r(\underline{x}) = \underline{\underline{S}}(\underline{x}) : (\underline{\underline{\sigma}}^r(\underline{x}) - \underline{\underline{\sigma}}^p(\underline{x})) \quad (10)$$

with

$$\langle \underline{\underline{\sigma}}^r(\underline{x}) \rangle_{\Omega} = \underline{\underline{0}} \quad (11)$$

Because of (8), one can write

$$\langle \underline{\underline{\epsilon}}^r(\underline{x}) \rangle_{\Omega} = \langle {}^t \underline{\underline{B}}(\underline{x}) \rangle_{\Omega} : \langle \underline{\underline{\epsilon}}^r(\underline{x}) \rangle_{\Omega} \quad (12)$$

Since ${}^t \underline{\underline{B}}(\underline{x})$ is statically admissible with $\underline{\underline{I}}$ and $\underline{\underline{\epsilon}}^r(\underline{x})$ is compatible, through the use of Hill's lemma (Hill, 1963), (12) becomes

$$\langle \underline{\underline{\epsilon}}^r(\underline{x}) \rangle_{\Omega} = \langle {}^t \underline{\underline{B}}(\underline{x}) : \underline{\underline{\epsilon}}^r(\underline{x}) \rangle_{\Omega} \quad (13)$$

By substitution of (10) for $\underline{\underline{\epsilon}}^r(\underline{x})$ in (13), we have

$$\langle \underline{\underline{\epsilon}}^r(\underline{x}) \rangle_{\Omega} = \langle {}^t \underline{\underline{B}}(\underline{x}) : \underline{\underline{S}}(\underline{x}) : \underline{\underline{\sigma}}^r(\underline{x}) \rangle_{\Omega} - \langle {}^t \underline{\underline{B}}(\underline{x}) : \underline{\underline{S}}(\underline{x}) : \underline{\underline{\sigma}}^p(\underline{x}) \rangle_{\Omega} \quad (14)$$

and by applying Hill's lemma again to the statically admissible stress field $\underline{\underline{\sigma}}^r(\underline{x})$ and to the compatible strain field ${}^t \underline{\underline{B}}(\underline{x}) : \underline{\underline{S}}(\underline{x})$

$$\langle \underline{\underline{\epsilon}}^r(\underline{x}) \rangle_{\Omega} = \langle {}^t \underline{\underline{B}}(\underline{x}) : \underline{\underline{S}}(\underline{x}) \rangle_{\Omega} : \langle \underline{\underline{\sigma}}^r(\underline{x}) \rangle_{\Omega} - \langle {}^t \underline{\underline{B}}(\underline{x}) : \underline{\underline{S}}(\underline{x}) : \underline{\underline{\sigma}}^p(\underline{x}) \rangle_{\Omega} \quad (15)$$

Because $\underline{\underline{\sigma}}^r(\underline{x})$ is self-equilibrated (11), the overall strain $\underline{\underline{E}}^r$ is

$$\underline{\underline{E}}^r := \langle \underline{\underline{\epsilon}}^r(\underline{x}) \rangle_{\Omega} = - \langle {}^t \underline{\underline{B}}(\underline{x}) : \underline{\underline{S}}(\underline{x}) : \underline{\underline{\sigma}}^p(\underline{x}) \rangle_{\Omega} \quad (16)$$

This strain is the residual overall strain of Ω (i.e., after global unloading).

2.2. Application to foams with closed cells

We first consider a two-phase material for which a Levin-type (Levin, 1967; Zaoui, 1996) analysis may be developed. In what follows, $\langle \cdot \rangle_{\alpha}$, ($\alpha = 1, 2$), means spatial average over phase (α) and c means the volume

fraction of phase (2). From now, it is assumed that the compliance $\underline{\underline{S}}(\underline{x})$ can be considered as uniform within each phase (ν) and its corresponding value is $\underline{\underline{S}}_\alpha$. For our purpose, the pre-stress field is assumed to be a uniform hydrostatic one acting in phase (2) only

$$\underline{\underline{\sigma}}^p(\underline{x}) := -P^{\text{int}} \underline{\underline{\delta}}_2(\underline{x}) \quad (17)$$

where $\underline{\underline{\delta}}_2(\underline{x})$ is equal to $\underline{\underline{1}}$, the second-rank identity tensor, if $\underline{x} \in (2)$ and to $\underline{\underline{0}}$ otherwise, and P^{int} is devoted to be the intracellular overpressure (relative to the atmospheric pressure) in the sequel.

In this case, (16) can be turned into

$$\underline{\underline{E}}^r = c P^{\text{int}} \langle \underline{\underline{B}}(\underline{x}) : \underline{\underline{S}}(\underline{x}) \rangle_2 : \underline{\underline{1}} \quad (18)$$

Transposition of (18) and symmetry of the strain tensor and of the compliance $\underline{\underline{S}}$ give

$$\underline{\underline{E}}^r = c P^{\text{int}} \underline{\underline{1}} : \langle \underline{\underline{S}}(\underline{x}) : \underline{\underline{B}}(\underline{x}) \rangle_2 = c P^{\text{int}} \underline{\underline{1}} : \underline{\underline{S}}_2 : \langle \underline{\underline{B}}(\underline{x}) \rangle_2 \quad (19)$$

By expanding the relation (7) in terms of spatial averages per phase, one gets

$$\underline{\underline{S}}^{\text{hom}} = (1 - c) \underline{\underline{S}}_1 : \langle \underline{\underline{B}}(\underline{x}) \rangle_1 + c \underline{\underline{S}}_2 : \langle \underline{\underline{B}}(\underline{x}) \rangle_2 \quad (20)$$

From this relation and (8), $\langle \underline{\underline{B}}(\underline{x}) \rangle_2$ in (19) may be expressed in terms of $\underline{\underline{S}}^{\text{hom}}$, namely

$$\langle \underline{\underline{B}}(\underline{x}) \rangle_2 = \frac{1}{c} (\underline{\underline{S}}_2 - \underline{\underline{S}}_1)^{-1} : (\underline{\underline{S}}^{\text{hom}} - \underline{\underline{S}}_1) \quad (21)$$

such that (19) becomes

$$\underline{\underline{E}}^r = P^{\text{int}} \underline{\underline{1}} : \underline{\underline{S}}_2 : (\underline{\underline{S}}_2 - \underline{\underline{S}}_1)^{-1} : (\underline{\underline{S}}^{\text{hom}} - \underline{\underline{S}}_1) \quad (22)$$

If we assume local and global isotropy, we get from (4), (5) and (22)

$$\underline{\underline{E}} = \left\{ \frac{1}{3k^{\text{hom}}} \underline{\underline{\Sigma}}^{\text{sph}} + \frac{1}{2\mu^{\text{hom}}} \underline{\underline{\Sigma}}^{\text{dev}} \right\} + \frac{\frac{1}{k_2}}{\frac{1}{k_2} - \frac{1}{k_1}} \left(\frac{1}{3k^{\text{hom}}} - \frac{1}{3k_1} \right) P^{\text{int}} \underline{\underline{1}} \quad (23)$$

where k_α and μ_α are the bulk and shear moduli of phase (α), k^{hom} and μ^{hom} are the effective bulk and shear moduli, $\underline{\underline{\Sigma}}^{\text{sph}}$ and $\underline{\underline{\Sigma}}^{\text{dev}}$ are the spherical and deviatoric part of the second-rank order tensor $\underline{\underline{\Sigma}}$. If $\underline{\underline{\Sigma}} = \underline{\underline{0}}$, $\underline{\underline{E}}$ is equal to $\underline{\underline{E}}^r$. While the elastic moduli of each phase are known, it remains to determine the effective elastic moduli, which can be done by direct measurement or by using an adequate model.

It has been noted in Hervé and Zaoui (1993), and in Hervé and Pellegrini (1995) that foams with closed cells can be considered as similar to composite materials with a continuous matrix embedding dispersed inclusions by zeroing the inclusion moduli k_2 and μ_2 in the initial three-phase model (Christensen and Lo, 1979). The estimated effective bulk modulus of this porous three-phase model is

$$k^{\text{hom}} = \frac{4\mu_1 k_1 (1 - c)}{4\mu_1 + 3k_1 c} \quad (24)$$

By putting $k_2 = 0$ in (23), and by using (24), the residual strain of problem (P) is (with $\underline{\underline{\Sigma}} = \underline{\underline{0}}$)

$$\underline{\underline{E}} = \underline{\underline{E}}^r = \frac{c}{1 - c} \left(\frac{1}{3k_1} + \frac{1}{4\mu_1} \right) P^{\text{int}} \underline{\underline{1}} \quad (25)$$

or in terms of k_1 and ν_1 , the matrix Poisson ratio

$$\underline{\underline{E}}^r = \frac{c}{1 - c} \frac{1 - \nu_1}{2(1 - 2\nu_1)} \frac{1}{k_1} P^{\text{int}} \underline{\underline{1}} \quad (26)$$

3. Isothermal linear viscoelastic foam shrinkage

We consider a volume element of a foam with closed cells at constant and uniform temperature with a traction-free boundary ($\underline{\underline{\Sigma}} = \underline{\underline{0}}$). The matrix is assumed to obey linear, isotropic and non-ageing viscoelasticity. The matrix Poisson ratio ν_1 is supposed to be constant. The intracellular pressure is time-dependent and, in all that follows, is denoted by $P^{\text{int}}(t)$.

It can be easily seen that the proposed micromechanical modelling with a linear elastic matrix (Section 2) remains valid if the matrix is now assumed to obey a linear and non-ageing viscoelastic behaviour. According to Mandel's correspondence principle (Mandel, 1955), all the viscoelastic variables are linked by a set of equations identical to the set of equations in the elastic theory, provided that each multiplication operation is replaced by an adequate convolution operation. In this way, the residual overall time-dependent foam strain in (26) reads

$$\underline{\underline{E}}(t) = \mathcal{K} \mathcal{J}(t) * \frac{dP^{\text{int}}}{dt}(t) \underline{\underline{1}} = \mathcal{K} \left\{ \int_{-\infty}^t \mathcal{J}(t-u) \frac{dP^{\text{int}}}{du}(u) du + \sum_i \mathcal{J}(t-t_i) \llbracket P^{\text{int}} \rrbracket_i \right\} \underline{\underline{1}} \quad (27)$$

with

$$\mathcal{K} := \frac{c}{1-c} \frac{1-\nu_1}{2(1-2\nu_1)} \quad (28)$$

$\mathcal{J}(t)$ is the bulk creep compliance (convolution-inverse of the bulk relaxation modulus, $k_1(t)$), $\llbracket P^{\text{int}} \rrbracket_i$ is any pressure discontinuity occurring at time t_i , and $*$ denotes the Riemann-convolution product. The reference state is chosen to correspond to the state at demoulding, which implies that the elastically delayed deformation due to the expansion stage history is not taken into account. In consequence, any deformation is referred to the state at demoulding ($t = 0$).

As an example, we assume that the matrix compliance obeys (Koeller, 1984) a parabolic creep function

$$\mathcal{J}(t) := J_0 \left[1 + \frac{1}{\Gamma(1+\beta)} \left(\frac{t}{\tau} \right)^\beta \right] \mathcal{H}(t) \quad (29)$$

where β is a fractional coefficient ($0 \leq \beta \leq 1$), J_0 is the elastic compliance, τ is a retardation time Γ the Euler function and $\mathcal{H}(t)$ the unit-step function. When $\beta = 0$, the matrix is elastic and when $\beta = 1$, it behaves like a Maxwell model. For intermediate values, the matrix has unlimited parabolic creep (figure 4).

In the following, we put $c = 0.98$, $\nu_1 = 0.3$ and we arbitrary choose two intracellular pressures, the first one is given in figure 5 and the second one is a 'Gaussian'-like function $e^{-(t/\tau)^2}$. Both pressure histories are normalized with the initial pressure P_0 . By using (27), (28) and (29), one can compute (respectively figures 6 and 7) the strain $E(t)$ defined as $\underline{\underline{E}}(t) = E(t) \underline{\underline{1}}$ of this foam with traction-free boundary for fractional coefficients β varying from 0.0 to 0.5. Numerical integration in (27) as well as numerical values of the Euler function (29) were performed with MATHEMATICA (version 2.2). No mathematical difficulties were encountered. One can see that the main characteristic of the strain response lies in a continual variation that is directly connected with the model's unlimited creep.

A matrix compliance with limited creep could be simply introduced by using the classical Kelvin-Voigt model

$$\mathcal{J}_{KV}(t) := J_0^{KV} (1 - e^{-t/\tau_{KV}}) \mathcal{H}(t) \quad (30)$$

Figures 8 and 9 respectively show the associated foam shrinkage for the intracellular pressure defined in figure 5 and by the 'Gaussian'-like function. Both normalized strain curves rapidly converge to the limit value of $-\mathcal{K} \simeq -42.9$.

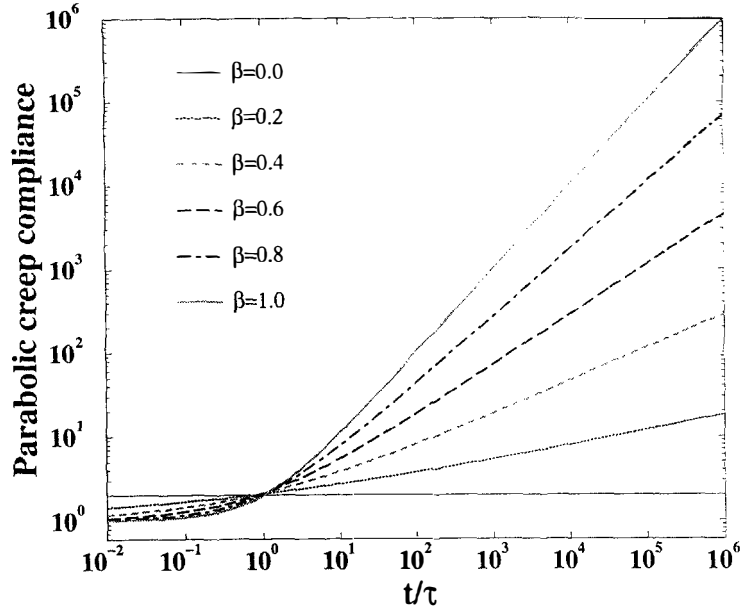


Figure 4. Normalized bulk creep compliance function $\frac{J(t)}{J_0}$ of the matrix (29).

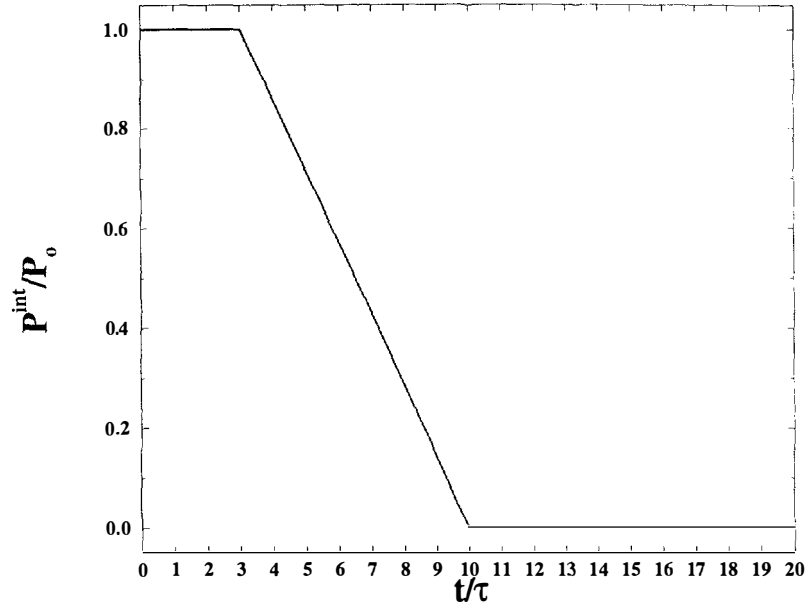


Figure 5. Normalized prescribed intracellular overpressure. The time-scale is also reduced with the retardation time of the matrix (29). The intracellular overpressure history before $t = 0$ (demoulding) is P_0 .

4. Non-isothermal viscoelastic shrinkage of an EPS bead

We consider an isolated expanded polystyrene bead which could be extracted from an EPS slab after demoulding. As mentioned in the introduction, both intracellular pressure and temperature variations must be taken into account for EPS time-dependent shrinkage after demoulding. From the end of moulding step, the

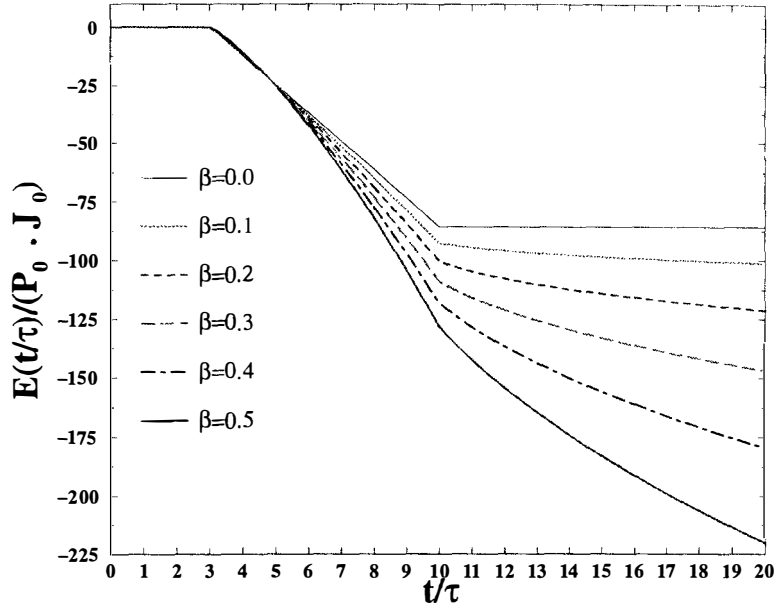


Figure 6. Normalized isothermal foam shrinkage for the intracellular pressure defined in figure 5. The initial state at time $t = 0$ is taken as the reference state.

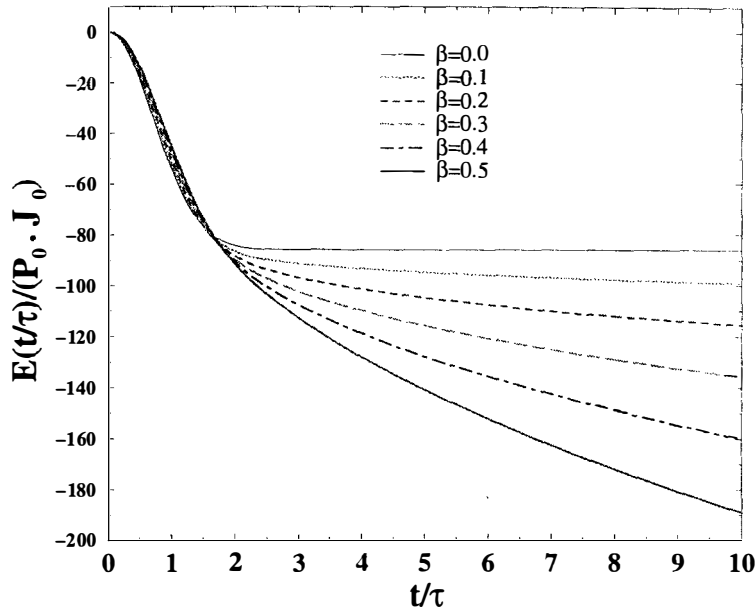


Figure 7. Normalized isothermal foam shrinkage for the 'Gaussian'-like intracellular pressure. The initial state at time $t = 0$ is taken as the reference state.

expanded bead is subjected to decreasing temperature and intracellular pressure. We assume that, at any constant temperature within a certain domain, the relation (27) is still valid

$$\underline{\underline{E}}_T(t) = \mathcal{K} \mathcal{J}_T(t) * \frac{dP^{\text{int}}}{dt}(t) \underline{\underline{1}} \quad (31)$$

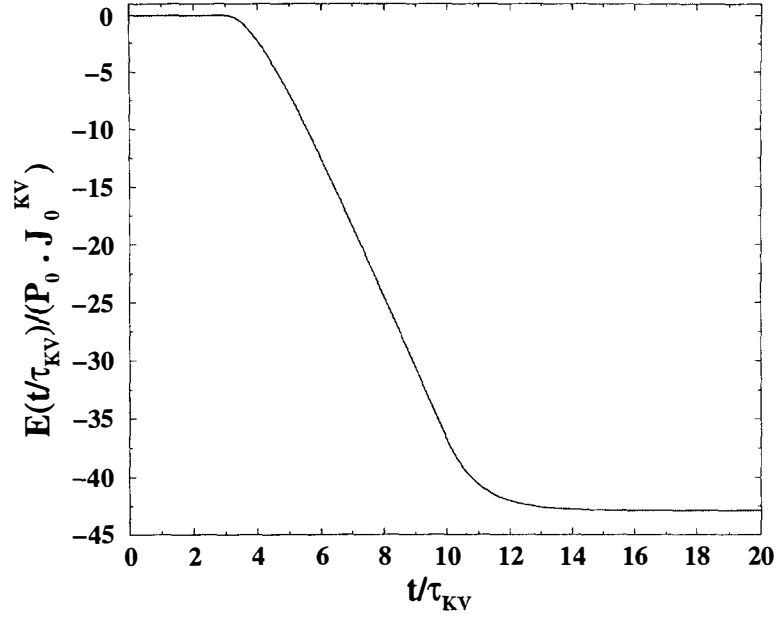


Figure 8. Normalized isothermal foam shrinkage for the intracellular pressure defined in *figure 5*. The initial state at time $t = 0$ is taken as the reference state. The matrix behaves as a Kelvin-Voigt model (30). The time-scale is reduced with the retardation time of the matrix (30).

where $\mathcal{J}_T(t)$ is the polystyrene bulk creep compliance at temperature T . In the following, we first present the chosen treatment before applying it to the case of an isolated EPS bead.

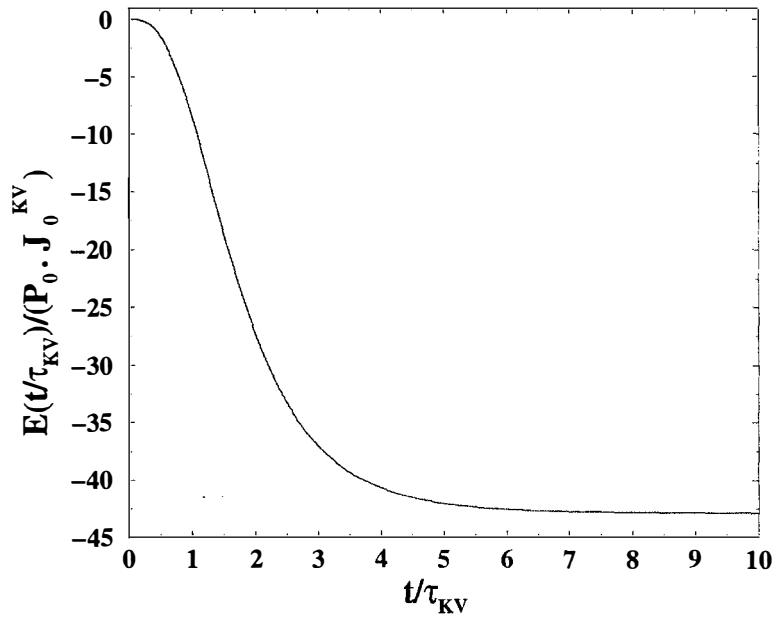


Figure 9. Normalized isothermal foam shrinkage for the ‘Gaussian’-like intracellular pressure. The initial state at time $t = 0$ is taken as the reference state. The matrix behaves as a Kelvin-Voigt model (30). The time-scale is reduced with the retardation time of the matrix (30).

4.1. Treatment of the non-isothermal viscoelastic response

The prediction of the mechanical response of a linear viscoelastic volume element under non-isothermal condition is still an open problem. This problem can be simplified if the material is assumed to obey the time-temperature equivalence principle. This consists in postulating that, at a constant temperature T , the variation of a given material property (such as the bulk creep compliance) during a time interval is equal to the one that results at a reference temperature T_r , during the same time interval divided by a temperature-dependent translation factor $a_{T_r}(T)$

$$\forall T, \quad \mathcal{J}_T(t) = \mathcal{J}_{T_r}(a_{T_r}(T)t) \quad (32)$$

The time-temperature equivalence principle is not sufficient for developing a non-isothermal theory. It only allows the prediction of the mechanical response of a material volume element at a constant temperature T if its behaviour is known at another temperature. A second hypothesis was originally put forward by Morland and Lee (1960) in connection with the time-temperature equivalence principle.

Its starting point is that if between t and $t + dt$, the temperature is $T(t)$, then the time-temperature equivalence principle yields $\mathcal{J}_T(t + dt - t) = \mathcal{J}_T(dt) = \mathcal{J}_{T_r}(a_{T_r}(T(t))dt)$. Thus the real time interval dt is equivalent to a modified one $d\xi = a_{T_r}(T(t))dt$. Let $T(t = 0) = T_r$, then $\mathcal{J}_T(0) = \mathcal{J}_{T_r}(0)$, such that

$$\xi := \mathcal{G}(t) = \int_0^t a_{T_r}[T(u)]du \quad (33)$$

Since, for all T , $a_{T_r}(T)$ is positive and continuous, then \mathcal{G} is continuous for all t and increases with time, such that its inverse function exists.

We can now introduce this second hypothesis to solve the non-isothermal viscoelastic problem. As proposed in Morland and Lee (1960), Muki and Sternberg (1961) and Christensen (1971), it consists of replacing the non-isothermal strain-stress constitutive relation by an isothermal linear viscoelastic strain-stress behaviour law with the modified time-scale ξ which accounts for the history of temperature.

Following this, the anisothermal problem constituted by (31) and by a given intracellular pressure and temperature histories is solved by the isothermal linear viscoelastic relation at T_r .

$$\underline{\underline{\hat{E}}}(\xi) := \mathcal{K} \mathcal{J}_{T_r}(\xi) * \frac{d\hat{P}^{\text{int}}}{d\xi}(\xi) \underline{\underline{1}} \quad (34)$$

where $\hat{f}(\xi)$ is defined by $f(t) := \hat{f}[\mathcal{G}(t)]$ and ξ is given by (33). The anisothermal viscoelastic strain is then computed by returning back to the t -real time-scale by inversion of the function \mathcal{G} .

This anisothermal strain must be completed with the thermal strain variation

$$\underline{\underline{E}}^{th}(t) = \alpha^{\text{hom}}(T(t) - T(0)) \underline{\underline{1}} \quad (35)$$

where α^{hom} is the overall linear thermal expansion coefficient of the EPS bead.

4.2. Application to an EPS bead

For illustration, we consider the following temperature history

$$T(t) := (T_i - T_f)e^{-(t/\theta)^2} + T_f \quad (36)$$

where T_i and T_f are respectively the initial and final temperatures and θ is a time-constant related to the temperature history. The given time-dependent temperature (36) is assumed to be close to that of a given point

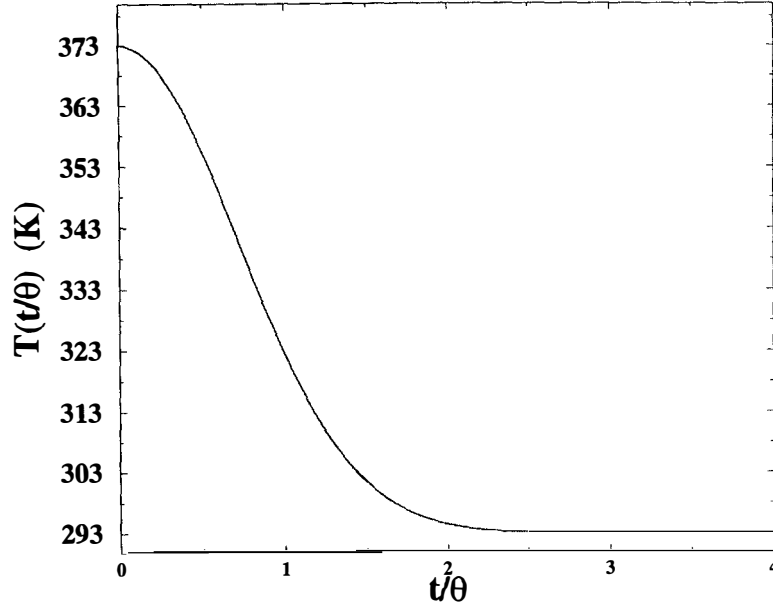


Figure 10. Temperature history, $T(t/\theta)$, from the end of the moulding step.

inside the EPS mould from the end of the moulding step, at $T_i = T_g \simeq 373$ K, to complete air-cooling, at $T_f \simeq 293$ K (see figure 10).

The intracellular pressure (figure 11) refers to the relative pressure exerted by the slab against the walls of the mould. Its amplitude $P_0 \simeq 1.2$ MPa. From experimental data, $t_2 \simeq 40$ hours whereas $t_1 \simeq 5$ seconds. In addition, t_2 corresponds to the time taken by the temperature to reach the ambient temperature, mostly because the intracellular pressure depends on temperature. One can see in figure 10 that the temperature nearly reaches

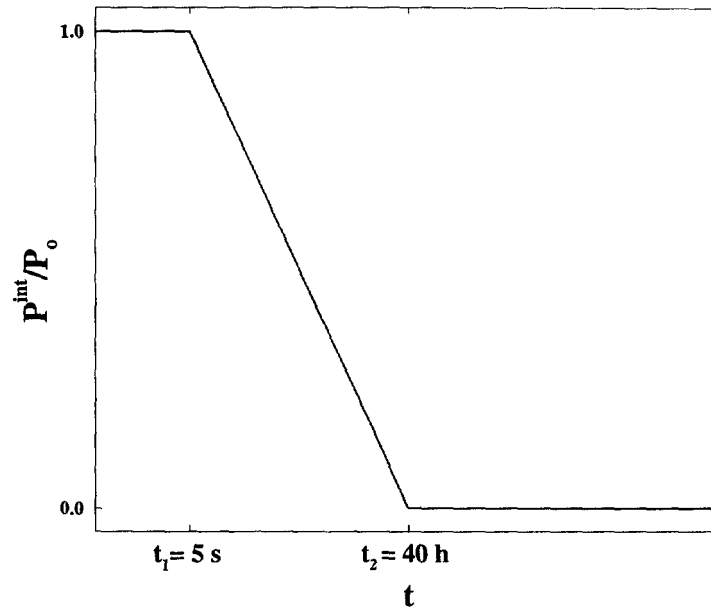


Figure 11. Intracellular overpressure history. P_0 is the initial pressure, t_1 and t_2 are two processing time-constants.

$T_f = 293$ K when $t/\theta \simeq 3$, such that $\theta \simeq 48000$ s. Thus, in what follows, $\theta = t_2/3$. This means that as soon as demoulding has begun, the intracellular pressure linearly decreases to the atmospheric pressure, while polystyrene becomes stiffer and stiffer since the temperature also decreases.

We assume that polystyrene is a linear viscoelastic material for temperature down to 293 K. This hypothesis is based on the existence of secondary molecular transitions at about and under 323 K for polystyrene (Yano and Wada, 1971) and on residual pentane content of the cell membranes of polystyrene after demoulding. These molecules separate the polymer chains from each other and hence create more free volume available for molecular motion (plasticization) effect (Cigna et al., 1986). Secondary transitions are associated with macromolecular motions concerning several monomers. Obviously, these molecular motions cannot explain high viscous deformations but could be responsible for small dimensional variations of EPS (less than about 1%) as typically observed during after-shrinkage.

Polystyrene is an amorphous polymer with a glass–rubber transition temperature of $T_g \simeq 373$ K. According to Halary (1995), such polymers obey the time–temperature equivalence principle from $T_g - 50$ K up to $T_g + 100$ K, i.e.. between 323 and 473 K for polystyrene. For our purpose, we assume that this domain can be extended down to 293 K. In the following, we still assume that the matrix Poisson ratio is constant. The shear and bulk creep compliances of the matrix are supposed to follow the time–temperature equivalence principle and, because of the constancy of the matrix Poisson ratio, they have the same translation factor a_{T_g} . Then, at each constant temperature T between 293 and 373 K, the relation (31) holds. The polystyrene bulk creep compliance $\mathcal{J}_T(t)$ is assumed to obey (29) with τ replaced by τ_T . Within the concerned temperature domain, the translation factor of polymers like polystyrene is said to be governed by an Arrhenius equation (Crum et al., 1988; Perez, 1992; Halary, 1995)

$$a_{T_g}(T) = e^{-\frac{\Delta H}{R}[\frac{1}{T} - \frac{1}{T_g}]} \quad (37)$$

where ΔH is the activation enthalpy of the molecular relaxation and R the gas constant $R \simeq 8.31 \text{ J.mol}^{-1}.\text{K}^{-1}$. It is reported (Crum et al., 1988) that $\Delta H \simeq 120 \text{ kJ.mol}^{-1}$ for glassy polymers under their glass-transition such that for polystyrene $\frac{\Delta H}{R.T_g} \simeq 39$.

Finally, the overall linear thermal expansion coefficient is calculated through Levin’s formula (Levin, 1967) applied to the ‘porous three-phase’ model. In this case, it is found to be identical to the linear thermal expansion coefficient of the matrix, that is $\alpha^{\text{hom}} = 8.10^{-5} \text{ K}^{-1}$ for glassy polystyrene (Sperling, 1992).

4.3. Results

With these values, the translation factor rapidly decreases to a low value at about $2.4.10^{-5}$ (*figure 12*), which means that at constant β , the creep curve at 373 K is shifted towards very much longer times (100 thousand times) when the temperature is lowered down to T_f .

The parameter J_0 of the parabolic hydrostatic creep compliance at T_g is set equal to 0.4 GPa^{-1} and assumed to be temperature-independent (following the time–temperature equivalence principle). This value corresponds to a polystyrene Young modulus of 3 GPa and a Poisson ratio of 0.3 at room temperature (typically 293 K) (Tobolsky, 1960; Sperling, 1992), and does not take the temperature-dependence of these elastic constants into account. If we take polystyrene viscosity at T_g to be about $\eta_g := 10^{13}$ Poise, which is the conventional value of viscosity at the glass–rubber transition, then we take the characteristic retardation-time of the creep compliance τ_g at T_g to be equal to $\tau_g := \frac{\eta_g}{k_1} = 400$ s. The reference temperature of (34) is $T_r := T_g$. Since $\theta \neq \tau_g$, a change of variable, $\omega(t/\theta) := \xi(t)/\theta$, is needed in (34). With the given intracellular pressure, *figure 11*, the

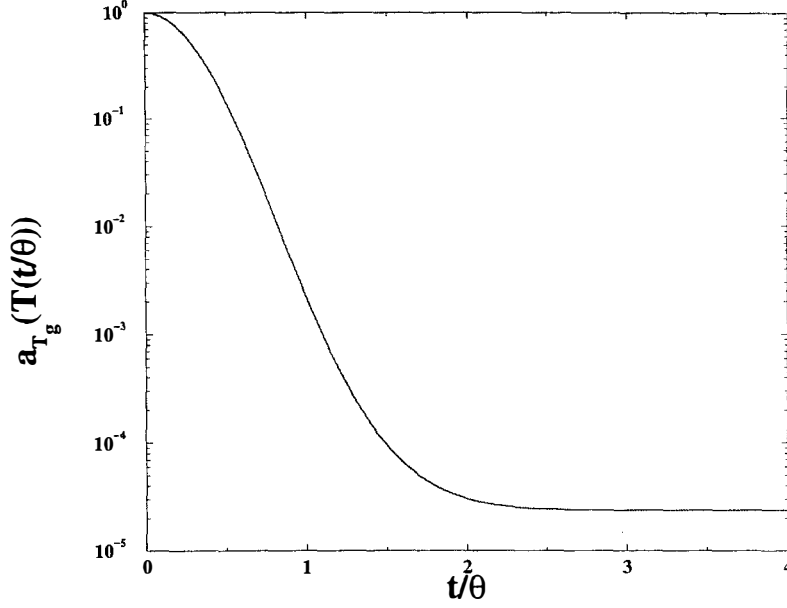


Figure 12. Translation factor versus time (Log-linear scale). It rapidly converges towards about $2.4 \cdot 10^{-5}$ with $\frac{\Delta T}{R \cdot T_g} = 39$.

fictitious isothermal strain at T_g becomes

$$\begin{aligned} \hat{\underline{\underline{E}}}(\theta\omega) = \frac{\mathcal{K}P_0J_0}{\omega_1 - \omega_2} & \left[(\omega - \omega_1)\mathcal{H}(\omega - \omega_1) - (\omega - \omega_2)\mathcal{H}(\omega - \omega_2) \right. \\ & \left. + \left(\frac{\theta}{\tau_g} \right)^\beta \frac{(\omega - \omega_1)^{1+\beta}\mathcal{H}(\omega - \omega_1) - (\omega - \omega_2)^{1+\beta}\mathcal{H}(\omega - \omega_2)}{\Gamma(1 + \beta)(1 + \beta)} \right] \underline{\underline{1}} \end{aligned} \quad (38)$$

where $\omega_i := \omega(t_i/\theta)$. By using the data given for polystyrene, the anisothermal deformation of the expanded bead is computed by inverting the function \mathcal{G} , on the reduced time-scale (t/θ) and then on the real time scale. Numerical evaluation of (38), of ω and ξ (33) is straightforwardly performed, while inversion of \mathcal{G} is evaluated by a first-order interpolation. All of them are performed with MATHEMATICA (version 2.2). *Figure 13* shows the simulated EPS bead shrinkage from the demoulding time on the real time-scale during 48 hours. It is worth noting that the expanded bead strain-rate at time t_1 is discontinuous as β approaches 0 from the right: if $\beta = 0$, $\dot{E}(t_1) = \frac{2\mathcal{K}J_0P_0}{t_1 - t_2}$ and if $\beta > 0$, $\dot{E}(t_1) = \mathcal{K}J_0P_0 \frac{a_{T_g}(t_1)}{\theta \int_{t_2/\theta}^{t_1/\theta} a_{T_g}(\theta u) du}$. Numerical evaluation yields a strain-rate of $\simeq -2.9 \cdot 10^{-7} \text{s}^{-1}$ for $\beta = 0$ and of $\simeq -1.4 \cdot 10^{-6} \text{s}^{-1}$ otherwise. Very high shrinkage amounts (up to 11.5% for $\beta = 0.5$) from demoulding are found and mostly take place during the first 10 hours. At this time the intracellular pressure is at about one-fourth of its final value and the temperature has decreased down to about 331 K (half its total variation amplitude), which means that these strain variations amplitudes and kinetics are mainly determined by high temperatures. *Figure 14* shows the EPS bead thermal strain: it is negligible with respect to the anisothermal strain due to the intracellular pressure variation shown in *figure 13*.

The influence of the absolute value of T_f on the simulated EPS bead strain variations are shown in *figure 15*. The thermal strain is not taken into account and, for simplicity, the matrix compliance follows the Kelvin–Voigt model (30): the retardation time at T_g and the elastic compliance J_0^{KV} are assumed to be the same as the previous ones (in the parabolic Maxwell model). Both intracellular pressure and temperature evolutions are identical to *figure 11* and to (36). In particular, the intracellular pressure reaches the atmospheric pressure when

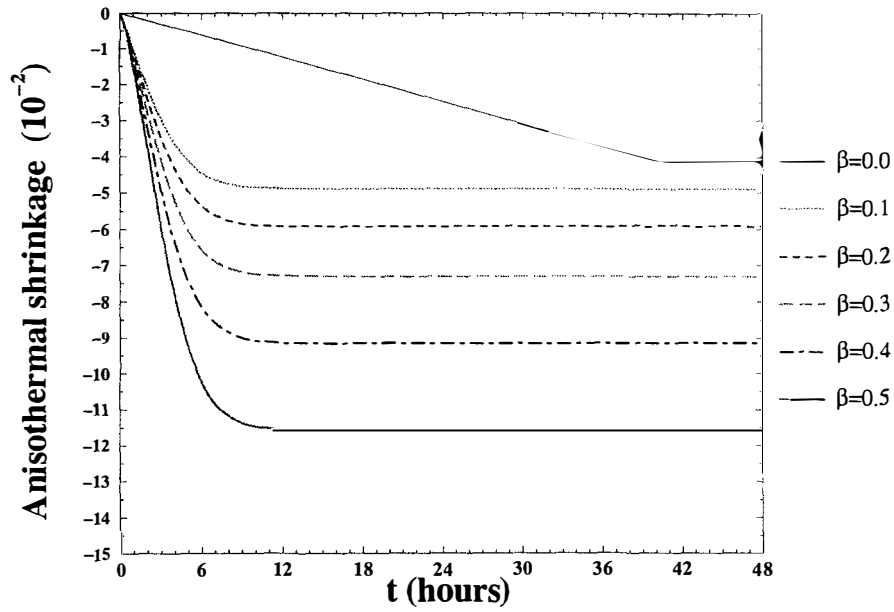


Figure 13. Foam shrinkage resulting from non-isothermal conditions just after demoulding.

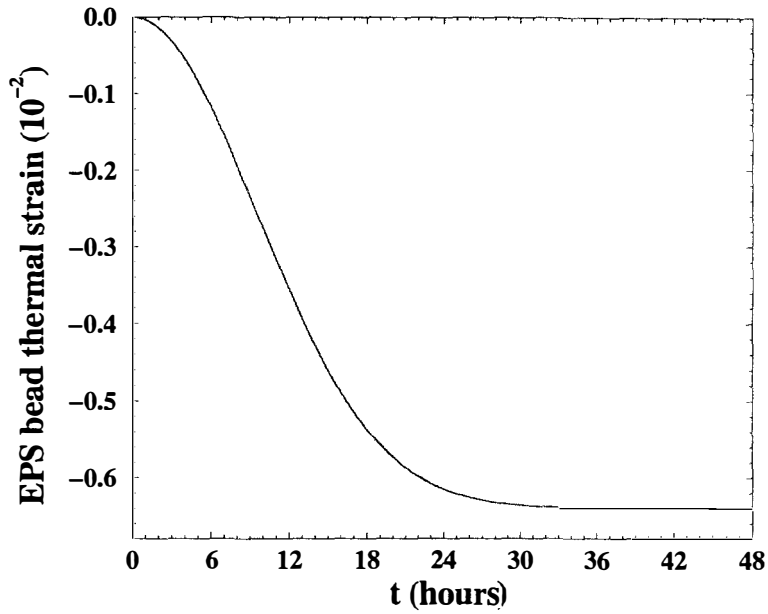


Figure 14. EPS bead thermal strain variation from the demoulding time.

the temperature reaches room temperature. As in the isothermal situation (*figures 8 and 9*), the strain rapidly converges to its limit value of $\mathcal{K}P_0J_0^{KV} \simeq -2.06\%$. The shrinkage rate is higher when T_f is decreased, which is not expectable at first. However, the shrinkage amplitude 40 hours after demoulding is higher with higher final temperature, which is substantial for the after-shrinkage. The thermal strain is again negligible with respect to the intracellular pressure-induced anisothermal strain.

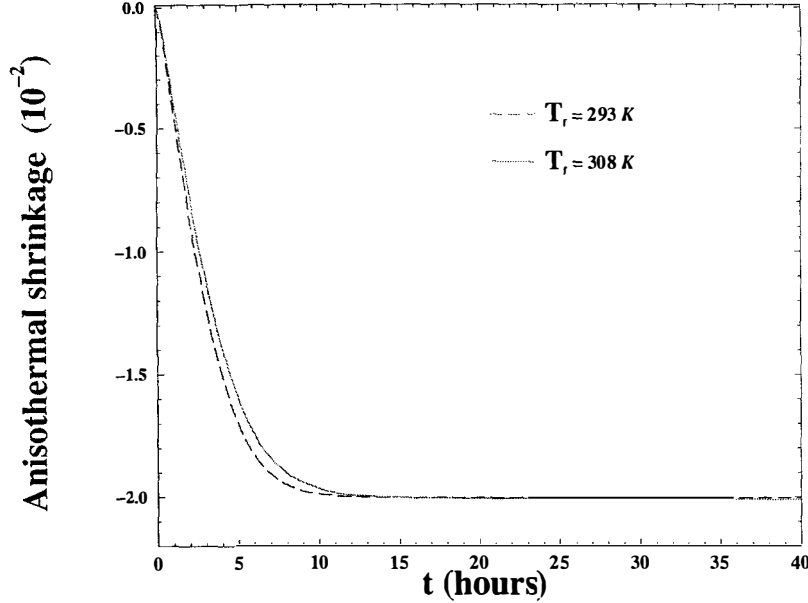


Figure 15. Foam shrinkage resulting from non-isothermal conditions after demoulding. The polystyrene matrix is assumed to obey the Kelvin-Voigt model (30). The initial temperature is 373 K for both cases.

5. After-shrinkage of EPS at room temperature

Expanded polystyrene variational dimensions have been shown to be harmful because they happen over quite a long time. Usually this is measured 24 hours after demoulding and is referred to as after-shrinkage. It is reported in Shell Plastics (1986) that an amplitude of more than 0.3 % can be observed for a 6-week after-shrinkage. In the following, after-shrinkage is estimated by translating the reference state of *figure 13* from $t = 0$ to $t = 24$ hours (*figure 16*) or to $t = 40$ hours (*figure 17*) and by taking into account the thermal strain. It is given by

$$\varepsilon(t) = \frac{E(t) - E(t_r)}{1 + E(t_r)} + \alpha^{\text{hom}}(T(t) - T(t_r)) \quad (39)$$

where t_r is the new reference state time. *Figure 16* shows an after-shrinkage evolution even for a purely elastic polystyrene ($\beta = 0$). This can be explained by relation (26): the elastic strain of a purely elastic bead is also time-dependent as long as the intracellular pressure varies with time: $\underline{\underline{E}}(t) = \mathcal{K}J_0P^{\text{int}}(t)\underline{\underline{1}}$.

At room temperature, the intracellular pressure has already reached the atmospheric pressure, such that it is impossible to explain EPS after-shrinkage at room temperature without the assumption of a viscoelastic behaviour for polystyrene. This is illustrated in *figure 17*: when polystyrene is purely elastic ($\beta = 0$), no variational dimensions are observed whereas an amplitude of more than 0.3 % ($\beta \geq 0.8$) can be obtained, which is in the range of order of the reported 6-week after-shrinkage amount (Shell Plastics, 1986). In fact, a wide range of after-shrinkage amplitudes could be predicted by changing the value of β or of the matrix Poisson ratio (for $\nu_1 = 0.5$, an amplitude of about 0.3 % is found for $\beta = 0.9$ instead of 0.8).

Figure 18 shows the EPS bead after-shrinkage for a Kelvin-Voigt matrix compliance and for two values of T_f . In contrast to the anisothermal shrinkage situation, higher final temperature allows after-shrinkage to be completed earlier because the retardation time is (slightly) higher at 308 rather than at 293 K. Unfortunately, the final temperature is the room temperature, which is weather-dependent and can hardly be controlled in order to shorten after-shrinkage duration. The after-shrinkage amplitude is also decreased with lower temperature, because 40 hours after demoulding the shrinkage at 293 K is further from its limit value than the shrinkage at 308 K

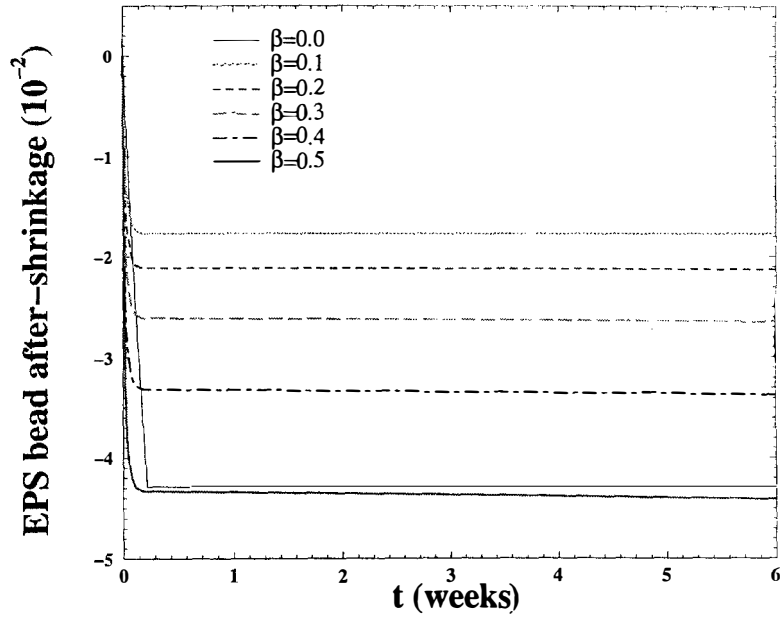


Figure 16. Foam after-shrinkage $\varepsilon(t)$ during 6 weeks. The reference state is the state 24 hours after demoulding.

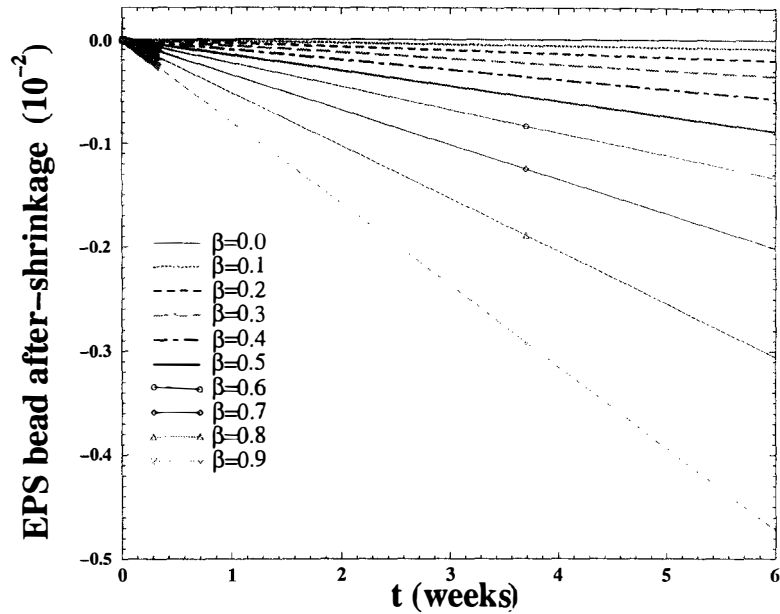


Figure 17. Foam after-shrinkage $\varepsilon(t)$ during 6 weeks. The reference state is the state 40 hours after demoulding. The temperature and intracellular pressure are now constant and respectively equal to 283 K and 1 atm.

[even though the limit values of the Kelvin–Voigt strain is the same for all temperatures, the after-shrinkage amplitude can be different if the reference state is different for different final temperatures; see Eq. (39)].

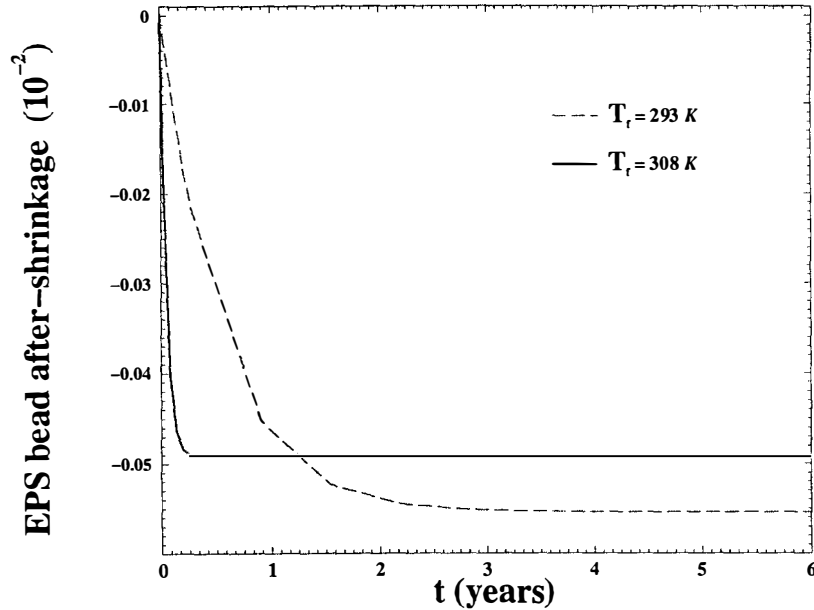


Figure 18. Foam after-shrinkage $\varepsilon(t)$ evolution for 6 years. The reference state is the state 40 hours after demoulding. The polystyrene matrix is assumed to follow the Kelvin–Voigt model (30). The intracellular pressure is now constant and equal to 1 atm and the thermal strain does not vary any more.

6. Conclusion

By assuming the homogeneity of the intracellular pressure inside the foam, an isotropic and homogeneous matrix material as well as global isotropy, it is possible to derive a micromechanical model for foams with closed pressured cells. This was first done in the linear theory of elasticity and non-ageing viscoelasticity and then in non-isothermal conditions with use of the time-temperature equivalence principle. The last case provides a qualitative explanation of the after-shrinkage of isolated expanded beads for two situations; the intracellular pressure is constant and there exists a small viscous part in the material behaviour of polystyrene at low temperature or polystyrene is linear elastic but the intracellular pressure is still decreasing. In other words, after-shrinkage of EPS slabs, due to that of the beads, can be due to the viscoelastic behaviour of polystyrene at room temperature associated with the intracellular pressure history before the time at which measurements have begun (see *figure 17*), or to a still decreasing intracellular pressure even though polystyrene would be purely elastic (see *figure 16*). The latter case is likely to generate high shrinkage amplitudes when shrinkage measurements start before EPS slabs reach complete air-cooling (in our example, 40 hours after demoulding).

Based on the restrictive adopted hypotheses, one way to reduce this time-lapse can be obtained by making thermal conduction and exchange with air easier in order to increase the cooling rate of EPS slabs. As far as after-shrinkage uniquely due to the viscoelastic behaviour of plasticized polystyrene is concerned, the only way would probably consists in making its kinetics the shortest as possible (by modifying the chemical composition of the cell membranes for instance).

Experimental studies are now in progress in order to determine the actual physical macromolecular motions responsible for viscoelasticity. Experimental refinements are also needed to quantitatively describe the thermomechanical behaviour of the cell membranes as well as the intracellular pressure. The thermomechanical study of an EPS slab will need to take the spatial heterogeneity of both temperature and intracellular pressure into account.

Acknowledgements

We are indebted to R. Da Silva (Lafarge-Plâtre) and to M. Lecomte (Shell) for information on EPS processing conditions. We are also grateful to T. Bretheau (LMS) for fruitful discussions.

References

- Christensen R., 1971, *Theory of Viscoelasticity*, Academic Press, New York.
- Christensen R., Lo K., 1979, Solutions for effective shear properties in three phase sphere and cylinder models, *J. Mech. Phys. Solids*, 27, 315–330.
- Cigna G., Merlotti M., Castellani L., 1986, Morphological and kinetic study of expandable polystyrene pre-expansion and effects on foam properties, *Cell. Polym.*, 5, 241–268.
- Crum N., Buckley C., Bucknall C., 1988, *Principles of Polymer Engineering*, Oxford Univ. Press, UK.
- Halary J., 1995, Traitement pratique des résultats des essais de viscoélasticité, in: G'sell C., Haudin J.M. (Eds), *Introduction à la mécanique des polymères*, Inst. Nat. Polytechnique de Lorraine, pp. 169–189.
- Hervé E., Pellegrini O., 1995, The elastic constants of a material containing spherical coated holes, *Arch. Mech.*, 47 (2), 223–246.
- Hervé E., Zaoui A., 1993, *n*-Layered inclusion-based micromechanical modelling, *Int. J. Eng. Sci.*, 31 (1), 1–10.
- Hill R., 1963, Elastic properties of reinforced solids: some theoretical principles, *J. Mech. Phys. Solids*, 11, 357–372.
- Järvelä P., Pohjonen T., Sarlin J., Törmälä P., Järvelä P., 1986, The after-shrinkage of expanded polystyrene and a method to eliminate it at the working temperature range, *Cell. Polym.*, 5, 289–301.
- Koeller R., 1984, Applications of fractional calculus to the theory of viscoelasticity, *J. Appl. Mech.*, 51, 299–307.
- Levin V., 1967, Thermal expansion coefficients of heterogeneous materials, *Mekh. Tverdogo Tela*, 2, 88–94; English translation, *Mech. Solids*, 11, 58–61.
- Mandel J., 1955, Sur les corps viscoélastiques à comportement linéaire, *C.R. Acad. Sci. Paris*, 241, 1910–1912.
- Morland L., Lee E., 1960, Stress analysis for linear viscoelastic materials with temperature variation, *Trans. Soc. Rheol.*, IV, 233–263.
- Muki R., Sternberg E., 1961, On transient thermal stresses in viscoelastic materials with temperature dependent properties, *J. Appl. Mech.*, 28, 193–207.
- Perez J., 1992, *Physique et mécanique des polymères amorphes*, Tech. and Doc-Lavoisier, Paris.
- Shell Plastics, 1986, *General Properties of Expanded Polystyrene*, Styrocell Tech. Manual, STY 5.1, 2nd edn.
- Sperling L., 1992, *Introduction to Physical Polymer Science*, John Wiley and Sons, NY.
- Tobolsky A., 1960, *Properties and Structure of Polymers*, John Wiley and Sons, NY.
- Yano O., Wada Y., 1971, Dynamic mechanical and dielectric relaxation of polystyrene below the glass temperature, *J. Polym. Sci.*, A-2, 9, 669–686.
- Zaoui A., 1996, *Matériaux hétérogènes et composites*, Presses de l'École Polytechnique, Palaiseau, France.